Ground fluidization promotes rapid running of a lightweight robot

Tingnan Zhang[1], Feifei Qian[1], Chen Li[1,2], Pierangelo Masarati[3], Aaron M. Hoover[2,4], Paul Birkmeyer[2], Andrew Pullin[2], Ronald S. Fearing[2] and Daniel I. Goldman[1]

Abstract

We study the locomotor mechanics of a small, lightweight robot (DynaRoACH, 10 cm, 25 g) which can move on a granular substrate of 3 mm diameter glass particles at speeds up to 5 body length/s, approaching the performance of certain desert-dwelling animals. To reveal how the robot achieves this performance, we used high-speed imaging to capture its kinematics, and developed a numerical multi-body simulation of the robot coupled to an experimentally validated simulation of the granular medium. Average speeds measured in experiment and simulation agreed well, and increased nonlinearly with stride frequency, reflecting a change in propulsion mode. At low frequencies, the robot used a quasi-static "rotary walking" mode, in which the substrate yielded as legs penetrated and then solidified once vertical force balance was achieved. At high frequencies the robot propelled itself using the speed-dependent fluid-like inertial response of the material. The simulation allows variation of parameters which are inconvenient to modify in experiment, and thus gives insight into how substrate and robot properties change performance. Our study reveals how lightweight animals can achieve high performance on granular substrates; such insights can advance the design and control of robots in deformable terrains.

1. Introduction

There is an increasing need for robots to traverse a diversity of complex terrain. Platforms have been developed that can effectively run on fractured rigid ground (Saranli et al., 2001; Schroer et al., 2004), crawl within concave surfaces (Wright et al., 2007), and climb on walls (Kim et al., 2007). However, relative to biological organisms (Li et al., 2012), human-made devices often have poor locomotor ability on granular substrates such as sand and gravel. For example, in wheeled and tracked vehicles, wheel slippage and sinkage can cause significant performance loss (Matson, 2010).

Granular media are collections of particles that interact through dissipative, repulsive contact forces (Jaeger et al., 1996). Forced granular media remain solid below the yield stress but flow like a fluid when the yield stress is exceeded (Nedderman, 2005). The solid–fluid transition presents great challenges for terrestrial devices moving on granular media. For example, previous studies (Li et al., 2009) demonstrated that a bio-inspired RHex-class legged robot, SandBot (30 cm, 2.3 kg), walked effectively at up to 1 body length/s on granular media at low to intermediate stride frequencies, where the granular material behaved like a yielding solid. The granular material yielded as the legs penetrated until vertical force balance was achieved. The granular material then solidified under the legs while the body lifted and moved forward, as if the robot were walking on a solid. At high stride frequencies, however, because the legs encountered previously disturbed ground, the granular material around the legs became continuously fluidized, and the robot "swam" forward slowly ($\sim$ 0.01 body length/s) using drag on the legs to overcome belly drag.

In contrast, a variety of animals live in the deserts and move rapidly across granular surfaces. For example, the zebra-tailed lizard (*Callisaurus draconoides*, $\sim$ 10 cm, $\sim$ 10 g) can run at speeds over 100 cm/s (10 body length/s) on sand. Unlike SandBot which must penetrate a large portion ($>$ 70%) of its limbs to move on granular media, the

[1]Georgia Institute of Technology, Atlanta, GA, USA
[2]University of California at Berkeley, Berkeley, CA, USA
[3]Dipartimento di Ingegneria Aerospaziale, Politecnico di Milano, Milano, Italy
[4]Franklin W. Olin College of Engineering, Needham, MA, USA

Corresponding author:
Daniel I. Goldman, Georgia Institute of Technology, 837 State Street, Atlanta, GA 30332, USA.
Email: daniel.goldman@physics.gatech.edu

Report Documentation Page				*Form Approved* *OMB No. 0704-0188*

Public reporting burden for the collection of information is estimated to average 1 hour per response, including the time for reviewing instructions, searching existing data sources, gathering and maintaining the data needed, and completing and reviewing the collection of information. Send comments regarding this burden estimate or any other aspect of this collection of information, including suggestions for reducing this burden, to Washington Headquarters Services, Directorate for Information Operations and Reports, 1215 Jefferson Davis Highway, Suite 1204, Arlington VA 22202-4302. Respondents should be aware that notwithstanding any other provision of law, no person shall be subject to a penalty for failing to comply with a collection of information if it does not display a currently valid OMB control number.

1. REPORT DATE **2013**	2. REPORT TYPE	3. DATES COVERED **00-00-2013 to 00-00-2013**

4. TITLE AND SUBTITLE **Ground fluidization promotes rapid running of a lightweight robot**	5a. CONTRACT NUMBER
	5b. GRANT NUMBER
	5c. PROGRAM ELEMENT NUMBER
6. AUTHOR(S)	5d. PROJECT NUMBER
	5e. TASK NUMBER
	5f. WORK UNIT NUMBER

7. PERFORMING ORGANIZATION NAME(S) AND ADDRESS(ES) **Georgia Institute of Technology,837 State Street,Atlanta,GA,30332**	8. PERFORMING ORGANIZATION REPORT NUMBER
9. SPONSORING/MONITORING AGENCY NAME(S) AND ADDRESS(ES)	10. SPONSOR/MONITOR'S ACRONYM(S)
	11. SPONSOR/MONITOR'S REPORT NUMBER(S)

12. DISTRIBUTION/AVAILABILITY STATEMENT **Approved for public release; distribution unlimited**

13. SUPPLEMENTARY NOTES

14. ABSTRACT

We study the locomotor mechanics of a small, lightweight robot (DynaRoACH, 10 cm, 25 g) which can move on a granular substrate of 3 mm diameter glass particles at speeds up to 5 body length/s, approaching the performance of certain desert-dwelling animals. To reveal how the robot achieves this performance, we used high-speed imaging to capture its kinematics, and developed a numerical multi-body simulation of the robot coupled to an experimentally validated simulation of the granular medium. Average speeds measured in experiment and simulation agreed well, and increased nonlinearly with stride frequency, reflecting a change in propulsion mode. At low frequencies, the robot used a quasistatic ?rotary walking? mode, in which the substrate yielded as legs penetrated and then solidified once vertical force balance was achieved. At high frequencies the robot propelled itself using the speed-dependent fluid-like inertial response of the material. The simulation allows variation of parameters which are inconvenient to modify in experiment, and thus gives insight into how substrate and robot properties change performance. Our study reveals how lightweight animals can achieve high performance on granular substrates; such insights can advance the design and control of robots in deformable terrains

15. SUBJECT TERMS					

16. SECURITY CLASSIFICATION OF:			17. LIMITATION OF ABSTRACT	18. NUMBER OF PAGES	19a. NAME OF RESPONSIBLE PERSON
a. REPORT **unclassified**	b. ABSTRACT **unclassified**	c. THIS PAGE **unclassified**	**Same as Report (SAR)**	**11**	

Standard Form 298 (Rev. 8-98)
Prescribed by ANSI Std Z39-18

lizard is light enough that even while running it only penetrates a small portion ($< 30\%$) of its limbs to generate force (Li et al., 2012). This suggests that a small, lightweight body may confer advantages for locomotion on deformable surfaces such as granular media.

Recent advances in the technique of smart composite microstructures (SCMs) (Wood et al., 2008) have enabled the development of small, lightweight robots ($\sim$ 10 cm, $\sim$ 20 g) (Hoover et al., 2010; Birkmeyer et al., 2009) such as DynaRoACH (Figure 1A). These robots are similar in size to the zebra-tailed lizard (and many other desert vertebrates and invertebrates (Mosauer, 1932; Crawford, 1981)) and can achieve performance approaching animals ($\sim$ 10 body length/s) on solid surfaces. Therefore, in addition to advancing locomotor capabilities of devices on complex terrain (Li et al., 2010), these lightweight robots provide promising physical models to study how effective legged locomotion can be achieved on granular (flowable) substrates in small, high-performing animals.

A challenge for studying locomotion on granular media is the lack of comprehensive force models at the level of the Navier-Stokes equations for fluids (Vogel, 1996). Recently an experimentally validated discrete element method (DEM) simulation (described below) of a model granular medium (3 mm diameter glass particles) was developed and successfully captured the locomotor mechanics of a sand-swimming lizard moving within granular media (Maladen et al., 2011). The DEM simulation provides a tool to obtain accurate, detailed information such as forces and flow fields of the media during intrusions relevant to locomotion. Such information is challenging to obtain in experiments, since force platforms (Biewener and Full, 1992) and 3D particle image velocimetry (PIV) techniques are not yet developed for deformable opaque ground.

In this paper we reveal principles of movement of lightweight locomotors on granular media using a combination of laboratory experiment and computer simulation. We perform studies of DynaRoACH on a medium of glass particles. To obtain estimates of ground reaction forces that result in high performance, we integrate the DEM simulation with a multi-body dynamic simulation of the robot. Our study reveals for the first time that qualitatively different propulsion mechanisms exist for low- and high-frequency movement on granular media. While the low-frequency locomotion of DynaRoACH can be understood using a previously introduced "rotary walking" model, at higher frequency, the robot utilizes the hydrodynamic response of the granular medium to achieve high performance through sustained fluidization of the ground. Furthermore, we use the simulation to systematically vary parameters such as friction (particle–particle and particle–leg) that are inconvenient to modify in experiment, and demonstrate performance and stability limits. We also investigate how limb width modifies the walk–run transition. We expect that the mechanics discovered here and the tools we have developed
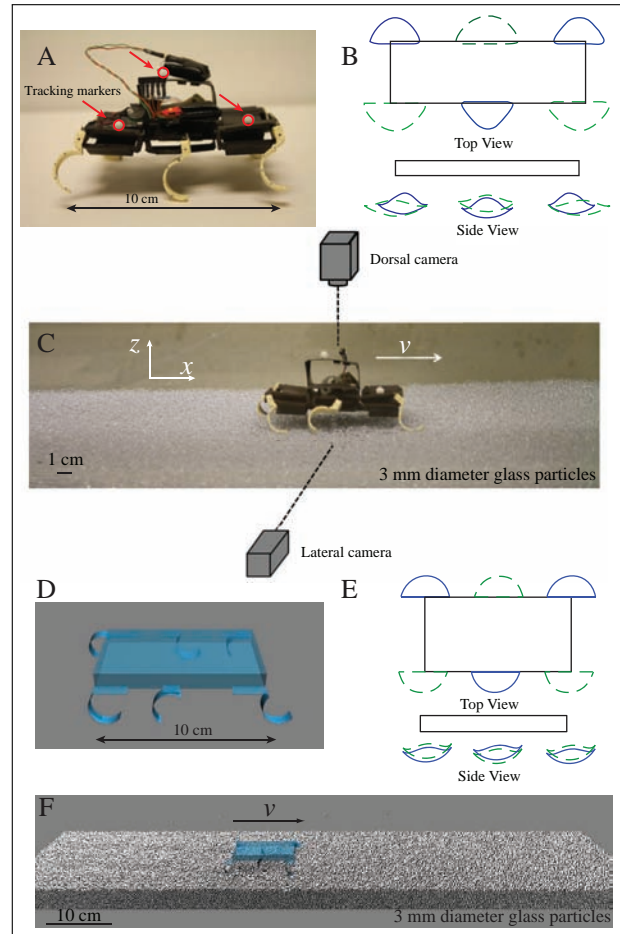

Fig. 1. Locomotion experiment and simulation. (A) The lightweight, hexapedal DynaRoACH robot resting on a bed of 3 mm diameter glass particles. (B) Leg tip trajectories from top view and side view. Solid blue and dashed green trajectories denote the two alternating tripods. (C) High-speed video experimental setup. (D) Simulation of the robot using MBDyn (E) Leg tip trajectories in simulation. (F) Simulation of the robot running on a bed of 3 mm particles (Extension 1).

should be applicable to other devices and provide a starting point to understand biological locomotion and develop robot designs on more complex deformable substrates, such as leaf litter and mud.

2. Materials and Methods

2.1. Experiments

2.1.1. Robotic platform The DynaRoACH robot used in this study (Figure 1A) is a small, lightweight (10 cm, 25 g), bio-inspired hexapedal robot (Hoover et al., 2010). It has six c-shaped legs (radius 1 cm) and runs with an alternating tripod gait. All six legs are driven by a single motor through body linkages. The motor is controlled by a centralized controller mounted close to the center of mass (CoM)

of the robot. Control parameters such as the stride frequency, running time, and PID control gains are set on a PC and communicated to the controller through a Bluetooth wireless interface.

2.1.2. Model granular media
We used 3.0 ± 0.2 mm diameter glass particles (density = 2.47 g/cm^3) as the granular medium (Figure 1C). The large size of the particles reduces computation time in the simulation portion of the study, facilitating a direct comparison between experiment and simulation. While these particles are larger than most natural sand grains, they have similar qualitative behavior in response to intrusion; a previous study (Maladen et al., 2011) also demonstrated that these particles provided a good model material for studying locomotion (swimming) within granular media.

In nature, granular media exist in a range of compactions, measured by the volume fraction ϕ (the ratio between the solid volume and the occupied volume). For dry granular media, ϕ can vary in the range $0.57 < \phi < 0.64$ (Dickinson and Ward, 1994), although this range is influenced by particle friction (Jerkins et al., 2008). The yield strength of a granular medium generally increases with ϕ (Li et al., 2009; Gravish et al., 2010) and affects locomotor performance on the granular medium (Li et al., 2009). In our study, we prepared the granular medium into a closely packed state ($\phi = 0.63$). However, we found that our results did not qualitatively change for different ϕ (e.g. robot speed was insensitive to ϕ), likely because the robot penetrated its legs into the granular medium to depths of only a few particle diameters and the range of achievable ϕ was small ($0.61 < \phi < 0.63$) in the low-friction 3 mm particles.

2.1.3. Locomotion experiments
We ran the DynaRoACH robot on a 75 cm long, 30 cm wide trackway filled with the 3 mm diameter glass particles to a depth of 6 cm (Figure 1C). We pressed the particles using a flat plate before each trial to prepare the particles to a closely packed state. Running kinematics were captured by two high-speed video cameras (AOS X-PRI) from both top and side views at a frame rate of 200 fps. One high-contrast dorsal marker was bonded above the robot CoM to obtain average forward speed; two lateral markers were bonded on the front and rear of the robot body to obtain CoM height (approximated by the average vertical position of the two markers). Stride frequency was determined from the videos.

2.1.4. Leg trajectories
To capture prescribed leg trajectories, the robot was suspended in the air and the trajectories of the leg tips were recorded as the motor rotated. During a cycle, each leg rotated backward about the hip (retraction), lifted-up sideways, and swung forward (protraction) (Figure 1B). Leg kinematic parameters such as the fore–aft swing angle and lateral lifting angle were determined by tracking the markers on the legs and used to guide tuning of leg trajectories in simulation. We define a stride period T as the time between the start of two consecutive retraction phases, and stance as when the leg generates ground reaction force (determined from simulation).

2.2. Simulation

2.2.1. DEM to model contact forces
To investigate locomotion of DynaRoACH in more detail, a simulation of the robot was developed and coupled to a granular media simulation. This granular simulation used the DEM to compute the particle–particle and particle–leg interactions for the 3 mm diameter glass particles. As in previous work (Maladen et al., 2011), the DEM simulation was validated by matching the forces on intruders moving in the granular medium (e.g. a rod dragged horizontally) with experimental measurements. In the DEM simulation, the normal contact force between an interacting pair of particles is given by a standard force law (Shäfer et al., 1996), a Hertzian repulsion and a velocity dependent dissipation (to account for a coefficient of restitution):

$$F_n = k_n \delta^{3/2} - g_n v_n \delta^{1/2}; \qquad (1)$$

the tangential contact force is modeled as Coulomb friction:

$$F_s = \mu F_n \qquad (2)$$

where δ is the deformation (virtual overlap) between contacting particle pairs or particle–leg pairs, v_n is the normal component of relative velocity, $k_n = 2 \times 10^6$ kg $\cdot$ s$^{-2} \cdot$ m$^{-1/2}$ and $g_n = 15$ kg $\cdot$ s$^{-1} \cdot$ m$^{-1/2}$ the contact stiffness and viscoelasticity dissipation coefficient, and $\mu_{\{pp,pl\}} = \{0.1, 0.3\}$ the particle–particle and particle–leg friction coefficients. The restitution and friction coefficients were experimentally measured and validated in a rod drag experiment (Maladen et al., 2011). Once the parameters were set in the DEM simulation, the robot locomotion could be accurately predicted over a wide range of conditions. The simulated granular bed (3×10^5 particles) was 60 PD (particle diameters) in width, 15 PD in depth, and 290 PD in length, and had frictionless boundaries (Figure 1F). At low frequencies we used a shorter granular bed (90 PD) containing 1×10^5 particles to save computation time.

2.2.2. Dynamic simulation of the robot
To model the robot we used a multi-body dynamic simulator, MBDyn (Ghiringhelli et al., 1999; Benedict et al., 2011), which allows time domain simulation of multi-body mechanical systems from first principle equations. MBDyn features a full 3D simulation with six translational and rotational degrees of freedom. This is essential for locomotion on the surface during which pitch, roll, and yaw are often present (Li et al., 2010).

In the dynamic simulation, the robot was constructed with similar body and leg geometries as the actual robot (Figure 1D). The simulated robot was composed of 13 individual rigid parts: one box-shaped body, six c-shaped legs,

and six linking plates between legs and body. The legs of the actual robot were not perfectly rigid but experimental observations showed little leg deformation during locomotion on granular media. The joints between the link plates and c-shaped legs allowed front–back swing of the legs while the plate–body joints allowed sideways lifting of the legs. Tuning kinematic parameters for the joint movements produced leg trajectories (Figure 1E) that resembled experimental measurements (Figure 1B) without mimicking the internal linkage of the actual robot.

2.2.3. Integration of DEM with dynamic simulation We combined MBDyn with the DEM code to simulate robot locomotion on granular media via a communication interface (a UNIX socket using C++). At each time step, MBDyn integrated the equations of motion for the robot combined with the forces and torques calculated from the DEM code. The updated kinematics including position, orientation, velocity, and angular velocity of each part of the robot were then passed back to the DEM code to compute the forces and torques on all interacting elements at the next time step. The time step was 2.5 μ sec , although setting it to 1 μ sec did not change the results; the time step was determined by typical particle overlap times in DEM.

In addition to the kinematics during locomotion (e.g. CoM position and velocity, stride length, limb penetration depth), the dynamics during locomotion (e.g. net ground reaction force on each limb and tripod) were also determined from the simulation.

2.2.4. Kinematic predictions based on previous work Because the small DynaRoACH robot has similarly shaped c-legs to the larger SandBot, we use the rotary walking model developed for SandBot (Li et al., 2009) to make two kinematic predictions for the locomotion of the DynaRoACH robot on granular media. We will test these predictions in both experiment and simulation.

First, we predict that both the body height and forward speed will increase during stance and decrease between stances. For walking at low frequencies, leg intrusion speeds will be small enough that granular forces will be dominated by friction, and therefore independent of speed, increase proportionally with depth (hydrostatic-like) (Albert et al., 1999; Hill et al., 2005). Once a result, during each step, the legs will initially slowly penetrate into granular medium while the body rests on the surface. Once the legs penetrate deeply enough for the lift on the legs to balance the weight and vertical inertial force of the body, the legs should stop penetrating and rotate atop solidified granular media, lifting the body and kinematically propelling it forward. As the legs withdraw from the granular medium, the body should fall and forward speed will decrease to zero. We refer to this as rotary walking in SandBot, and expect to see these features in the small robot.

Second, based on the rotary walking model, we predict that stride length should decrease with stride frequency. In the quasi-static rotary walking mode, stride length is inversely related to leg penetration depth by geometry. As stride frequency increases, because the inertial force required for body lift-up increases, the legs should penetrate more deeply, and therefore the stride length should decrease. In addition, the transition from walking to swimming should be triggered by the reduction in stride length: at high enough stride frequency, stride length should become small enough that the legs will encounter previously disturbed material during each step.

3. Results and discussion

3.1. Kinematics

From measurements in simulation of the instantaneous speed of the robot (see Fig. 2), we computed time-averaged forward speed. The speed of the robot measured in both experiment and simulation (Figure 3A) agreed well, and increased monotonically with stride frequency. At the highest stride frequency tested in experiment (12 Hz), the robot reached a speed of 50 cm/s (5 body length/s), comparable to slow runs of the zebra-tailed lizard. Calculated stride length (Figure 3B) decreased with stride frequency from low (0–3 Hz) to intermediate frequencies (4–6 Hz) but increased with stride frequency at high frequencies (7–12 Hz). Duty factor (the percentage of the total stride period during which the limb is in contact with the ground) measured in simulation (Figure 2E and J) fell below 0.5 at intermediate frequencies of $\sim$ 6 Hz (Figure 3C), indicating the onset of aerial phases. Closer examination of the kinematics revealed that the robot displayed a transition in locomotor mode as stride frequency increased.

3.1.1. Walking at low stride frequencies At low stride frequencies (e.g. 3 Hz, Figure 2A–E and Extension 2), as predicted, the DynaRoACH robot used a quasi-static rotary walking locomotor mode, where forward speed increased sub-linearly with stride frequency (i.e. stride length decreased; Figure 3B). Instantaneous forward speed also increased from 0 to 25 cm/s during most of stance and then dropped to zero (Figure 2C). Vertical position of the CoM simulation (Figure 2B and D) showed that average body height was 1.28 ± 0.03 cm during stance, increased by 0.46 ± 0.03 cm (38% of the standing body height 1.2 cm) during most of stance, and then decreased by the same amount.

The observed decrease in stride length with stride frequency, increase in body height and forward speed during most of stance, and decrease in body height and forward speed between stances were in accord with predictions of the rotary walking model (Li et al., 2009) (Figure 3A and 3B, red curve). This suggests that like SandBot, the
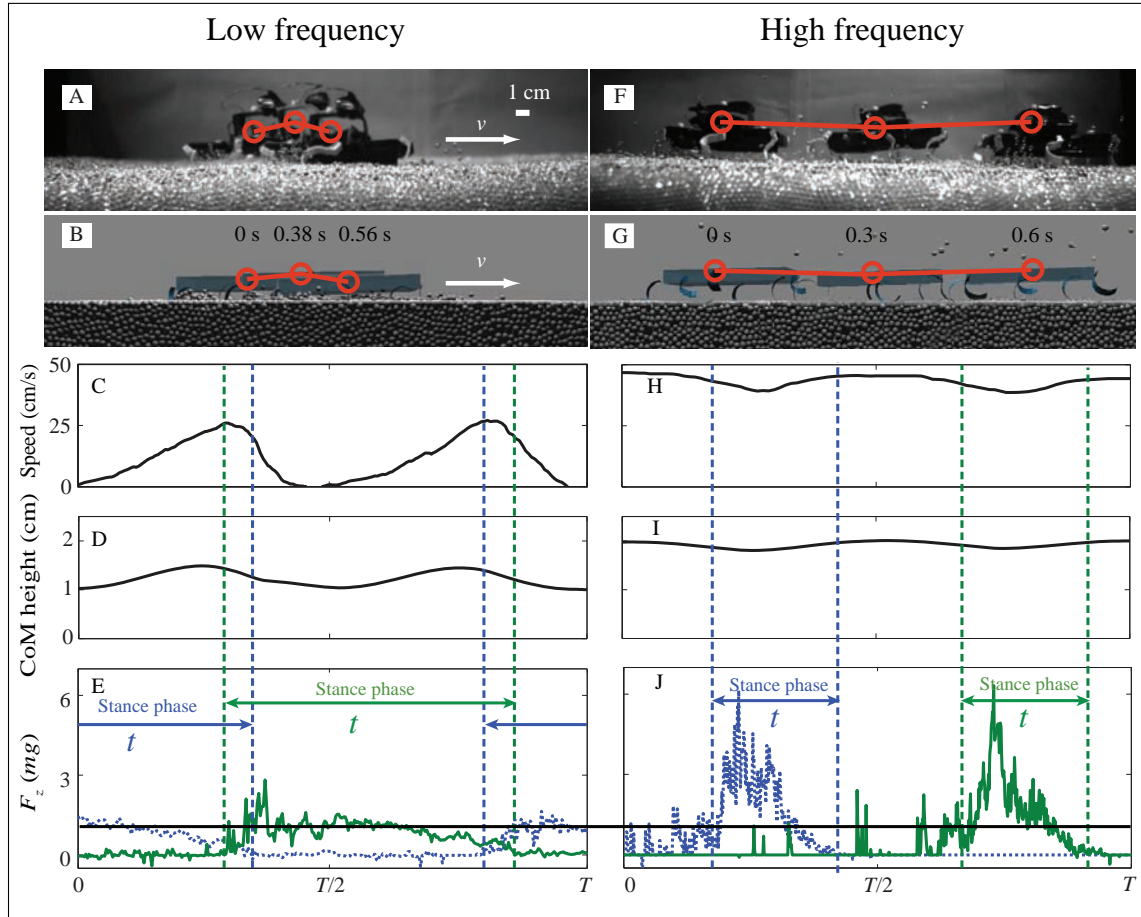
Fig. 2. Two locomotion modes observed for the robot moving on granular media: (A)–(E) walking at low frequencies (e.g. 3 Hz); (F)–(J) running at high frequencies (e.g. 11 Hz). (A), (F) Sideview of the robot in experiment. (B), (G) Sideview of the robot in simulation. (C), (H) Instantaneous forward speed versus time. (D), (I) Body height versus time. (E), (J) Vertical ground reaction force on a tripod versus time. Dashed blue curve and solid green curve are for the two alternating tripods. Black horizontal line indicates body weight (*mg*). In (A), (B) and (F), (G) the three time instants shown are the start, middle, and end of three different stances. In (C)–(E) and (H)–(J) data are shown for simulation only. Duty factor is stance duration *t* divided by stride period *T*.

small DynaRoACH robot also rotary-walked on solidified granular media at low frequencies.

The decrease in body height and forward speed occurred at the start of stance; however, this does not contradict the rotary walking model, but is a consequence of the different leg trajectories of the small robot and SandBot. Because SandBot rotates its legs in circular trajectories, its body must rest on the surface between two tripods, resulting in stance phase that begins during the retraction phases of legs. The DynaRoACH robot instead uses protraction–retraction leg trajectories, which result in stance phases that begin during protraction phases of the legs.

3.1.2. Running at high stride frequencies At high stride frequencies (Figure 2F–J, 11 Hz, and Extension 2) the DynaRoACH robot exhibited a different locomotor mode than that predicted by the rotary walking model. The forward speed of DynaRoACH increased super-linearly

with stride frequency (i.e. stride length increased; Figure 3B). Instantaneous forward speed was always greater than zero and decreased during the first half of stance. It then increased during the second half of stance (Figure 2H). The average body height measured in simulation was 1.86 ± 0.02 cm above the surface (Figure 2F, G, I), which was 0.58 cm (48% of the standing body height 1.2 cm) higher than that at low frequencies. Body height decreased by 0.19 ± 0.02 cm (16% of the standing body height 1.2 cm) during the first half of stance and increased by the same amount during the second half of stance. Simulation revealed that grains around the intruding legs remained fluidized throughout the stance phase.

While these kinematics were different from those predicted by the rotary walking model (Figure 3A and B, red curve), they also differed from the slow surface swimming which SandBot used at high stride frequencies (Li et al., 2009), in which the body height remained constant while the belly lay on the surface and forward speed was small

(~ 1 cm/s). For DynaRoACH running on granular media at high frequencies, we observed a decrease in body height and instantaneous forward speed during the first half of stance, a monotonic increase of average forward speed with stride frequency, and aerial phases observed. These signatures were also observed in the zebra-tailed lizard running on granular substrates (Li et al., 2012); that study revealed that the lizard's movement could be described by a spring-loaded inverted pendulum (SLIP) model (Blickhan, 1989). This similarity suggested that unlike SandBot, but like the zebra-tailed lizard, the small robot used a SLIP-like running mode on granular media at high frequencies.

3.2. Vertical ground reaction force

To understand the mechanism of the transition in locomotor mode from walking at low frequencies to running (but not swimming) at high frequencies, we examined in simulation the vertical ground reaction force, F_z, on a tripod of legs. For animals and legged robots moving on deformable or yielding substrates such as the surface of water (Glasheen and McMahon, 1996) or granular surfaces (Li et al., 2009, 2012), it is critical that the material generates sufficient F_z to balance the weight and inertial force of the body before legs sink too deeply into the substrate. Averaged over a cycle, lift must equal the body weight, i.e. $\frac{1}{DT} \int F_z dt = mg$, where mg is the body weight of the robot, T the cycle period, and D the duty factor defined as the stance duration divided by T.

At low stride frequencies (e.g. 3 Hz), because duty factor was greater than (but close to) 0.5, F_z on both tripods was close to the body weight for most of the cycle (Figure 2E). As duty factor decreased below 0.5 with increasing stride frequency, F_z on both tripods no longer overlapped, and the magnitude of F_z on each tripod increased. The peak of F_z increased from $\sim 1\ mg$ at 3 Hz (Figure 2E) to $\sim$ 6–7 mg at 12 Hz (Figure 2J). Peak torque on a tripod about the hips measured in simulation at 12 Hz was 10 mN-m; this was less than the stall torque of the motor–gearbox system.

The rotary walking model can only explain the mechanism governing the increase in F_z at low frequencies. At low frequencies ($<$ 3 Hz), the granular force is friction-dominated, and therefore is independent of intrusion speed and increases with penetration depth. As stride frequency increased, this depth-dependent granular force increased due to the increasing inertial force associated with the lifting of the body (Li et al., 2009); this resulted in an increasing penetration depth (Figure 4A). As stride frequency increased to $>$ 3 Hz, however, the measured leg penetration depth decreased (Figure 4A), counter to the prediction of the rotary walking model. In this regime the walking model also predicted a decrease in the lift force on the legs, contrary to observations (Figure 2E and J).

This discrepancy suggests that there must be additional contribution to the force at high frequencies. Examination
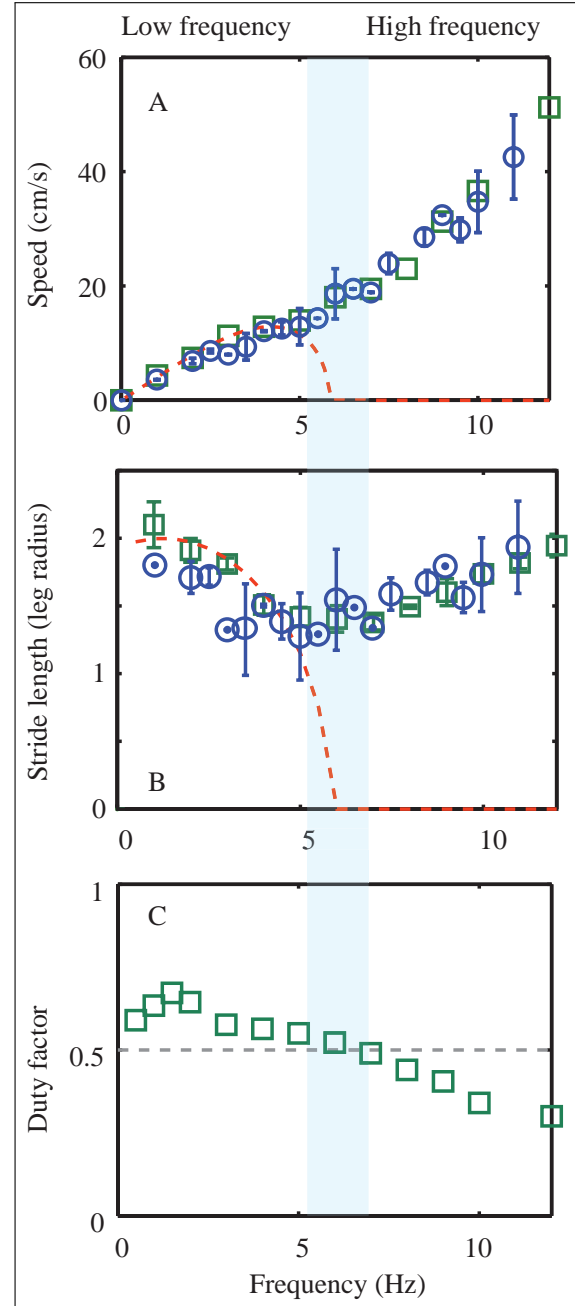

Fig. 3. Performance and gait parameters (blue circles: experiment; green squares: simulation): (A) average forward speed versus stride frequency; (B) stride length versus stride frequency; (C) duty factor versus stride frequency (simulation only). Blue region indicates where transition of locomotor mode occurs. Dashed red curves in (A, B) are predictions from the rotary walking model (Li et al., 2009). Error bars indicate standard deviation.

of leg kinematics in simulation revealed that the vertical penetration speed of the legs increased with stride frequency and reached nearly 1 m/s at 12 Hz (Figure 4B). It is known that the granular forces during high-speed impact are hydrodynamic-like and increase approximately quadratically with impact speed (Katsuragi and Durian, 2007;
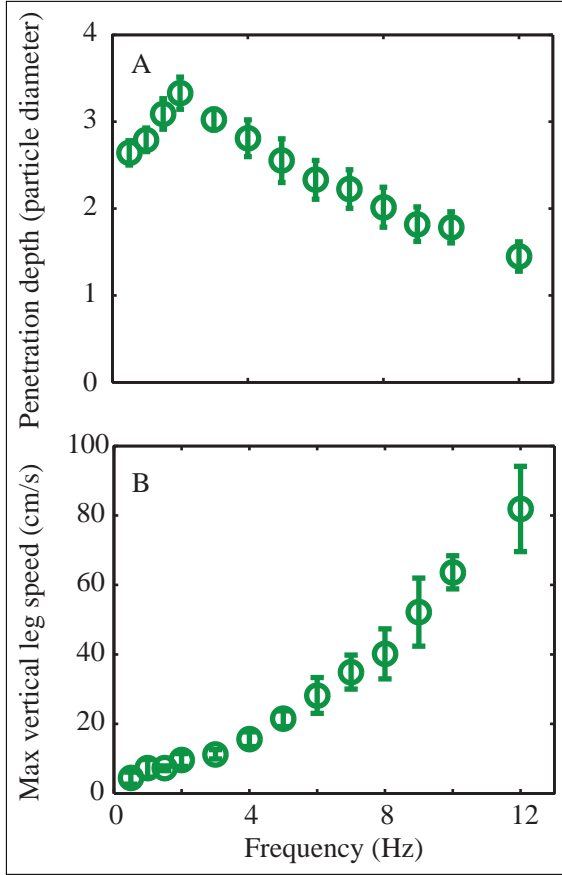
Fig. 4. Limb penetration and intrusion speed measured in simulation. (A) Maximum leg penetration depth (measured in particle diameters) versus stride frequency. (B) Maximum leg vertical penetration speed versus stride frequency. Error bars indicate standard deviation.
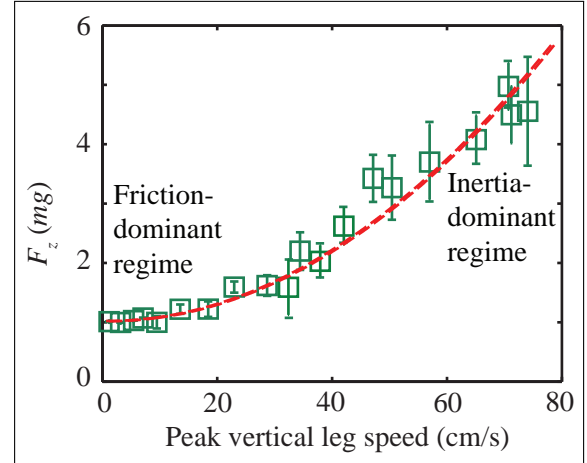

Fig. 5. Vertical ground reaction force versus maximum leg penetration speed. Dashed red curve indicates quadratic fit $F_z/mg = \alpha v^2 + 1$ with fitting parameter $\alpha = 5.7 \times 10^{-3}$ cm^{-2}s^2. Error bars indicate standard deviation.

Goldman and Umbanhowar, 2008). Our data of lift versus vertical leg penetration speed (Figure 5, green squares) can be described approximately by a quadratic with a non-zero *y*-intercept (Figure 5, dashed red curve), due to the finite yield stress of the medium. We hypothesize that as the vertical leg penetration speeds increases, the inertial force of the grains being accelerated by the legs becomes important and contributes significantly to the vertical ground reaction force. In other words, at high frequencies, the robot runs on granular material that behaves like an inertial fluid, much like the basilisk lizard (*Basiliscus*), the so-called "Jesus lizard" that runs on the surface of water (Glasheen and McMahon, 1996).

We used previous intrusion studies in granular media to estimate the transition frequency for the DynaRoACH robot. Studies of horizontal drag and vertical impact in granular media (Albert et al., 1999; Katsuragi and Durian, 2007; Goldman and Umbanhowar, 2008) suggest that inertial effects become important for intrusion speeds beyond $v_c \sim (2gd)^{1/2}$, where *d* is the particle diameter and *g* the gravitational acceleration. For 3 mm glass particles,

$v_c = 25$ cm/s. This indicates that hydrodynamic-like force should become significant as the vertical leg penetration speed increases beyond ~ 25 cm/s, or as stride frequency increases past ~ 6 Hz (Figure 4B). This is in accord with the observed transition in locomotor mode around 6 Hz (Figure 3). We posit that this transition of the propulsion mechanism from low-frequency (i.e. low vertical penetration speed) walking on yielding ground to high-frequency (i.e. high vertical penetration speed) running on fluidizing ground is generic to locomotion on granular media. However, the frequency at which the walk-to-run transition occurs should depend on parameters associated with the granular media as well as the robot morphology and kinematics.

The capability of the small robot to run rapidly at high frequencies on granular media by using hydrodynamic-like forces, in contrast to SandBot's slow swimming, suggests that lightweight locomotors have an advantage when moving on granular surfaces. Indeed, the small robot's legs are relatively large (projected surface area ~ 1.4 cm^2) compared with its body weight (25 g) (each leg of a tripod applies a pressure of 600 Pa when standing), and can generate enough hydrodynamic-like lift by paddling its legs rapidly to maintain the body well above the surface. By contrast, SandBot's legs are relatively small (projected surface area ~ 5 cm^2) compared with its body weight (2300 g) (each leg of a tripod applies a pressure of $\sim 1.5 \times 10^4$ Pa when standing), and cannot generate enough hydrodynamic-like lift to support the body before the legs sink deeply enough to encounter previously disturbed material over steps and trigger swimming. This may explain why the zebra-tailed lizard, the highest-performing among desert lizards of similar size, has the largest hind feet (Li et al., 2012).

4. Parameter variation and broader applicability

Because the MBDyn multi-body simulation is based on first principles (i.e. Newton–Euler equations of motion), and the DEM simulation of granular media is based on validated empirical models (e.g. Hertzian contact theory, Coulomb model of friction), our results should be applicable to a broad class of granular substrates. The simulation tool therefore allows rapid and accurate systematic variation of the properties of the locomotor (e.g. leg morphology, leg kinematics) as well as the granular substrate (e.g. size, density, friction, and hardness of particles). For example, while in experiment it is difficult to alter only one property while not changing others, in simulation we can test the effects of each substrate property. This can provide insight for design of future multi-terrain robots, and allows testing of biological hypotheses. To demonstrate the capabilities of our simulation for parameter variation, we varied the coefficients of particle–particle friction μ_{pp}, particle–leg friction μ_{pl}, and leg width, and tested the effects of these parameters on the robot speed.

4.1. Friction coefficients

Dramatic changes in locomotor performance were observed when μ_{pp} was varied (Figure 6A). For walking at low frequencies (e.g. 3 Hz, Figure 6A, filled green squares), the robot speed increased monotonically with μ_{pp}, and saturated at high μ_{pp}. In this regime, forces were dominated by friction (particularly, μ_{pp}). As μ_{pp} increased, the legs needed to penetrate less to balance body weight and inertial forces. As a result, stride length and speed increased with μ_{pp}. The saturation of speed at high μ_{pp} was a consequence of leg penetration depth approaching zero with increasing μ_{pp}. Thus, stride length could not increase further.

For running at high frequencies (e.g. 12 Hz, Figure 6A, empty green squares, and Extension 3), the robot speed increased with μ_{pp} for $\mu_{pp} < 0.2$ and decreased with μ_{pp} for $\mu_{pp} > 0.2$. The increase of speed with μ_{pp} for $\mu_{pp} < 0.2$ is likely because the inertial force provided by the particles being accelerated by the legs increased with μ_{pp}. We observed that multiple layers of particles directly under and around the legs were fluidized during leg penetration. We hypothesize that the size of the region of accelerating particles increases with μ_{pp} because larger μ_{pp} facilitates interlocking of the particles. The decrease of speed with μ_{pp} between $0.2 < \mu_{pp} \lesssim 0.4$ for running at high frequencies is likely a result of reduction in propulsion due to an asymmetric gait. We observed that in this regime, the particles became more tightly interlocked and lost fluidity. The lift force on one tripod alone became sufficient to accelerate the robot up such that the body traveled in the air during the remainder of the cycle and the other tripod never touched the ground.

As μ_{pp} increased above ~ 0.4, the particles became so tightly interlocked that the granular substrate behaved like
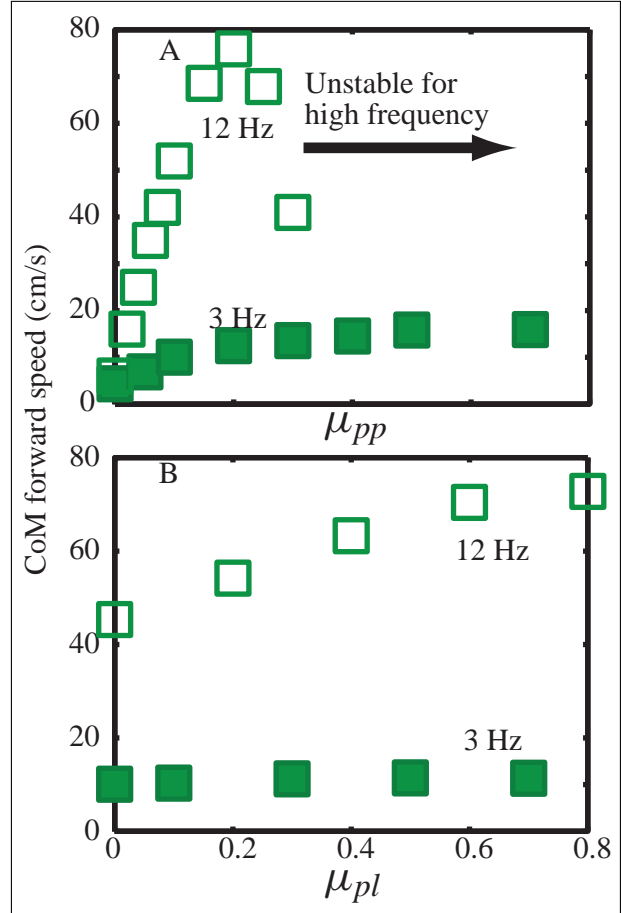

Fig. 6. Robot average forward speed upon variation of (A) particle–particle friction μ_{pp} (with $\mu_{pl} = 0.3$) and (B) particle–leg friction μ_{pl} (with $\mu_{pp} = 0.1$) in simulation (filled green squares: 3 Hz; empty green squares: 12 Hz).

rigid ground. Locomotion became unstable as the robot bounced erratically, and its movement direction changed randomly. This is similar to the unstable motion of the robot on rigid ground (Li et al., 2010). Forward speed was not well defined in this regime. The perfectly rigid legs of the robot used in simulation may have contributed to this instability by generating force spikes during substrate impact (Kim et al., 2006).

Particle–leg friction μ_{pl} had little effect on the robot speed at low frequencies (e.g. 3 Hz, Figure 6B, filled squares). We observed that the penetration depth and the stride length remained the same when μ_{pl} increased. This indicates that the yielding forces of granular media during low-speed penetration are insensitive to the surface roughness of the c-legs, but instead are dominated by particle–particle friction (Figure 6A). We hypothesize that at low frequencies, as the robot rotary walks on solidified particles, ground reaction force results primarily from normal forces on the leading surface (rather than friction on the thin sides) of the c-legs.
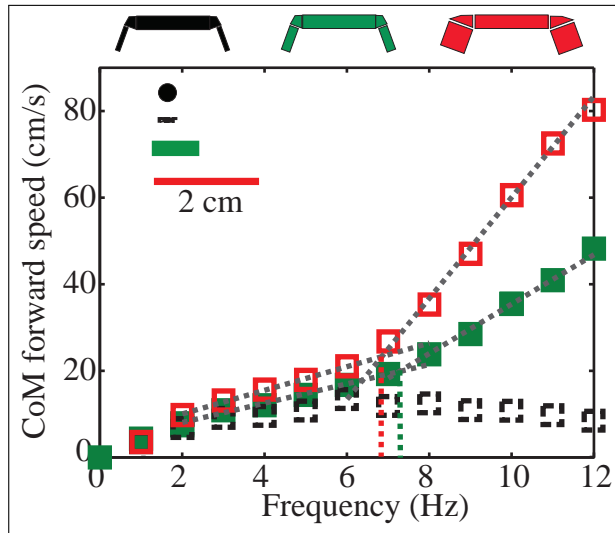
Fig. 7. Robot average forward speed versus stride frequency (solid green squares: original foot width of 0.7 cm; dashed black squares: foot width of 0.3 cm; empty red squares: foot width of 2 cm) for different leg widths (in simulation). Horizontal bars in the inset represent the width of the legs. The filled black circle indicates the particle size. Front view of the robot with different leg widths are shown on top. Values of friction coefficients $\mu_{\{pp,pl\}} = \{0.1, 0.3\}$ are used. The dashed lines in the 2 cm and 0.7 cm leg widths are separate linear fits to the speed of the robot between the stride frequencies of 2–6 Hz and 7–12 Hz. The intersection of a pair of lines indicates the transition frequency from rotary-walking-dominated locomotion to fluid-like propulsion.

At high frequencies (e.g. 12 Hz, Figure 6B, empty squares) the robot speed was sensitive to (and increased with) μ_{pl}. We observed an increase in F_x but not F_z with μ_{pl} (e.g. F_x increased by 50% when μ_{pl} increased from 0 to 0.7 while F_z did not change significantly). Further work is needed to better understand propulsive force in the high-frequency impact-induced fluid-like regime.

4.2. Leg morphology

Because both hydrostatic-like frictional forces (Albert et al., 1999; Hill, et al., 2005) and hydrodynamic-like inertial forces (Katsuragi and Durian, 2007; Goldman and Umbanhowar, 2008) are proportional to intruder area, we expected that an increase (or decrease) of the robot leg width would result in increased (or decreased) ground reaction forces. To test how leg size affects locomotor performance and transitions in locomotor modes, in simulation we varied the width of all the six c-legs (Figure 7, top diagrams) while keeping their radius and kinematics fixed.

At low stride frequencies (1–3 Hz) the performance of the robot was insensitive to changes in the leg morphology (Figure 7). Because the robot is lightweight, at low frequencies the stride length was near $2r$, the maximal value of the stride length for rotary walking (where r is the leg radius), seen in the original legs (Figure 3B). An increase in the foot width could not increase the stride length significantly beyond $2r$ and thus the forward speed did not increase significantly (Figure 7, filled green squares to empty red squares). When the width of the legs was close to the particle diameter, we postulated that the ground reaction force would no longer linearly scale with the leg area. In the low-frequency regime we observed that the penetration depth increased by only 33% when the foot width was reduced to half of the original width. As a result, the stride length and speed did not drop substantially (Figure 7, filled green squares to dashed black squares).

In contrast, at high stride frequencies the robot's performance depended sensitively on the leg width. We observed that increasing the leg width by 3 times (from 0.7 cm to 2.0 cm) increased the stride length (and, thus, the average speed) by up to 1.7 times (Figure 7, from filled green to empty red). Surprisingly, the frequency at which the robot switched from rotary-walking behavior to fluid-like propulsion was insensitive to leg width. We determined the transition frequencies from the intersection of linear fits to the speed of the robot in two regions, 2–6 Hz and 7–12 Hz (Figure 7, dotted gray lines). We found that the transition frequencies decreased by only ~ 0.5 Hz (about 6%) when the leg width increased by 3 times. Transition frequencies measured from duty factor (i.e. the frequency at which duty factor = 0.5) also showed a decrease by ~ 1 Hz ($\sim 10\%$). This implies that the relationship between foot area and average speed is non-trivial. We hypothesize that it is governed by a nonlinear interplay of body inertia and complex intrusion rheology. Advances in the physics of intrusion and impact (Clark et al., 2012; Seguin et al., 2013; Li et al., 2013) are required to develop a fundamental understanding of such interactions.

In addition, decreasing the leg width by 50% (from 0.7 cm to 0.3 cm) (Figure 7, filled green to dashed black) resulted not only in decreased speeds at low frequencies, but also triggered a transition of locomotor mode from running to slow swimming (similar to that observed in SandBot (Li et al., 2009)).

5. Conclusion

Inspired by high-performing desert animals moving on granular media, we studied in experiment the locomotion of a lightweight, bio-inspired, legged robot (DynaRoACH) on a granular substrate and developed an experimentally validated computer simulation of the locomotion. Our approach enabled examination of the mechanics responsible for the robot's high locomotor performance. DynaRoACH displayed a transition in locomotor mode from walking at low frequencies to running at high frequencies. At low frequencies, hydrostatic-like forces generated during yielding of the granular material ultimately led to solidification of the material, and the robot moved as if it were walking on a solid surface. At high frequencies, however, the inertia of the grains being accelerated became important and

forces became hydrodynamic-like. In this regime the robot ran rapidly by paddling legs on fluidized granular material. Thus our results reveal that lightweight robots can achieve high locomotor performance on granular media by exploiting the fluid-like properties of these substrates.

The experimentally validated simulation of the lightweight robot platform provides the most accurate model to date of robot locomotion on granular media, and therefore enables detailed examination of the mechanics of legged locomotion over a wide range of flowable substrates. In particular, the simulation tool we have developed can be used to systematically test the effect of both locomotor and substrate properties on locomotor performance. Practically this can guide the design, control and power consumption estimates for high-performing multi-terrain robot platforms.

Finally, we note that while the approach described here allows detailed investigation of mechanics of movement, a complementary approach is needed: the development of low-order dynamical models (Li et al., 2013) that can be used to gain insight into the critical mechanics of dynamical running. In our future work, we will investigate whether a dynamic force relationship that describes the hydrodynamic-like forces during high-speed leg intrusions can be obtained from measurements in DEM simulation. We posit that a generalized locomotion model similar to the SLIP (Blickhan, 1989) can be developed based on such a force relationship and can extend our current study to more generalized conditions. This generalized model will shed light on the locomotor dynamics of legged animals and robots on granular media, as well as guide development for analytically tractable low-order models.

References

Albert R, Pfeifer MA, Barabási A-L and Schiffer P (1999) Slow drag in a granular medium. *Physical Review Letters* 82: 205–208. DOI: 10.1103/PhysRevLett.82.205.

Benedict M, Mattaboni M, Chopra I and Masarati P (2011) Aeroelastic analysis of a micro-air-vehicle-scale cycloidal rotor in hover. *AIAA Journal* 49: 2430–2443. DOI: 10.2514/1.J050756.

Biewener AA and Full RJ (1992) Force platform and kinematic analysis. *Biomechanics: Structures and Systems: A Practical Approach*. IRL Press at Oxford University Press, pp. 45–73.

Birkmeyer P, Peterson K and Fearing RS (2009) DASH: A dynamic 16g hexapedal robot. In: *IEEE/RSJ International Conference on Intelligent Robots and Systems, 2009 (IROS 2009)*, pp. 2683–2689. DOI: 10.1109/IROS.2009.5354561.

Blickhan R (1989) The spring-mass model for running and hopping. *Journal of Biomechanics* 22: 1217–1227. DOI: 10.1016/0021-9290(89)90224-8.

Clark AH, Kondic L and Behringer RP (2012) Particle scale dynamics in granular impact. *Physical Review Letters* 109: 238302. DOI: 10.1103/PhysRevLett.109.238302.

Crawford CS (1981) *Biology of Desert Invertebrates.* New York: Springer.

Dickinson WW and Ward JD (1994) Low depositional porosity in eolian sands and sandstones, Namib Desert. *Journal of Sedimentary Research* 64: 226–232. DOI: 10.1306/D4267D66-2B26-11D7-8648000102C1865D.

Ghiringhelli GL, Masarati P, Mantegazza P and Nixon MW (1999) Multi-body analysis of a tiltrotor configuration. *Nonlinear Dynamics* 19: 333–357. DOI: 10.1023/A:1008386219934.

Glasheen JW and McMahon TA (1996) A hydrodhynamic model of locomotion in the basilisk lizard. *Nature* 380: 340–342. DOI: 10.1038/380340a0.

Goldman DI and Umbanhowar PB (2008) Scaling and dynamics of sphere and disk impact into granular media. *Physical Review E* 77: 021308. DOI: 10.1103/PhysRevE.77.021308.

Gravish N, Umbanhowar PB and Goldman DI (2010) Force and flow transition in plowed granular media. *Physical Review Letters* 105: 128301. DOI: 10.1103/PhysRevLett.105.128301.

Hill G, Yeung S and Koehler SA (2005) Scaling vertical drag forces in granular media. *EPL (Europhysics Letters)* 72: 137. Doi:10.1209/epl/i2005-10203-3.

Hoover AM, Burden S, Fu X-Y, Sastry SS and Fearing RS (2010) Bio-inspired design and dynamic maneuverability of a minimally actuated six-legged robot. In: *3rd IEEE RAS and EMBS International Conference on Biomedical Robotics and Biomechatronics (BioRob), 2010*, pp. 869–876. DOI: 10.1109/BIOROB.2010.5626034.

Jaeger HM, Nagel SR and Behringer RP (1996) The physics of granular materials. *Physics Today* 49: 32. DOI: 10.1063/1.881494.

Jerkins M, Schröter M, Swinney HL, Senden TJ, Saadatfar M and Aste T (2008) Onset of mechanical stability in random packings of frictional spheres. *Physical Review Letters* 101: 018301. DOI: 10.1103/PhysRevLett.101.018301.

Katsuragi H and Durian DJ (2007) Unified force law for granular impact cratering. *Nature Physics* 3: 420–423. DOI: 10.1038/nphys583.

Kim S, Clark JE and Cutkosky MR (2006) iSprawl: Design and tuning for high-speed autonomous open-loop running. *The International Journal of Robotics Research* 25: 903–912. DOI: 10.1177/0278364906069150.

Kim S, Spenko M, Trujillo S, Heyneman B, Mattoli V and Cutkosky MR (2007) Whole body adhesion: hierarchical, directional and distributed control of adhesive forces for a climbing robot. In *Proceedings IEEE International Conference on Robotics and Automation, 2007 (ICRA2007)*, pp. 1268–1273. DOI: 10.1109/ROBOT.2007.363159.

Li C, Hoover AM, Birkmeyer P, Umbanhowar PB, Fearing RS and Goldman DI (2010) Systematic study of the performance of small robots on controlled laboratory substrates. In: *Proceedings of SPIE* 7679, Micro- and Nanotechnology Sensors, Systems, and Applications II: 76790Z. DOI: 10.1117/12.851047.

Li C, Hsieh ST and Goldman DI (2012) Multi-functional foot use during running in the zebra-tailed lizard (*callisaurus draconoides*). *The Journal of Experimental Biology* 215: 3293–3308. DOI: 10.1242/jeb.061937.

Li C, Umbanhowar PB, Komsuoglu H, Koditschek DE and Goldman DI (2009) Sensitive dependence of the motion of a legged robot on granular media. *Proceedings of the National Academy of Sciences of the USA* 106: 3029–3034. DOI: 10.1073/pnas.0809095106.

Li C, Zhang T and Goldman DI (2013) A terradynamics of legged locomotion on granular media. *Science* 339: 1408–1412. DOI: 10.1126/science.1229163.

Maladen RD, Ding Y, Umbanhowar PB, Kamor A and Goldman DI (2011) Mechanical models of sandfish locomotion reveal principles of high performance subsurface sand-swimming. *Journal of The Royal Society Interface* 8: 1332–1345. DOI: 10.1098/rsif.2010.0678.

Matson J (2010) Unfree Spirit: NASA's Mars Rover appears stuck for good. *Scientific American* 302: 16. DOI: 10.1038/scientificamerican0410-16a.

Mosauer W (1932) Adaptive convergence in the sand reptiles of the Sahara and of California: A study in structure and behavior. *Copeia* 1932(2): 72–78.

Nedderman RM (2005) *Statics and kinematics of granular materials*. Cambridge: Cambridge University Press.

Saranli U, Buehler M and Koditschek DE (2001) RHex: A simple and highly mobile hexapod robot. *The International Journal of Robotics Research* 20: 616–631. DOI: 10.1177/02783640122067570.

Schroer RT, Boggess MJ, Bachmann RJ, Quinn RD and Ritzmann RE (2004) Comparing cockroach and Whegs robot body motions. In: *Proceedings 2004 IEEE International Conference on Robotics and Automation, 2004 (ICRA2004)*, vol. 4, pp. 3288–3293. DOI: 10.1109/ROBOT.2004.1308761.

Seguin A, Bertho Y, Martinez F, Crassous J and Gondret P (2013) Experimental velocity fields and forces for a cylinder penetrating into a granular medium. *Physical Review E* 87: 012201. DOI: 10.1103/PhysRevE.87.012201.

Shäfer J, Dippel S and Wolf DE (1996) Force schemes in simulations of granular materials. *Journal de Physique I France* 6(1): 5–20. DOI: 10.1051/jp1:1996129.

Vogel S (1996) *Life in Moving Fluids: The Physical Biology of Flow*. Princeton, NJ: Princeton University Press.

Wood RJ, Avadhanula S, Sahai R, Steltz E and Fearing RS (2008) Microrobot design using fiber reinforced composites. *Journal of Mechanical Design* 130: 052304. DOI: 10.1115/1.2885509.

Wright C, Johnson A, Peck A, Naaktgeboren A, Gianfortoni P, Gonzalez-Rivero M, Hatton RL and Choset H (2007) Design of a modular snake robot. In *IEEE/RSJ International Conference on Intelligent Robots and Systems, 2007 (IROS 2007)*, pp. 2609–2614. DOI: 10.1109/IROS.2007.4399617.

Appendix: Index to Multimedia Extensions

The multimedia extension page is found at http://www.ijrr.org

Table of Multimedia Extensions

Extension	Type	Description
1	Video	Simulation of DynaRoACH running on 3 mm particles
2	Video	Walking at low frequencies and running at high frequencies
3	Video	Effects of particle–particle friction coefficients on running at high frequencies